JOURNAL OF CATALYSIS 59, 248–262 (1979)

Infrared, Microcalorimetric, and Electron Spin Resonance Investigations of the Acidic Properties of the H–ZSM-5 Zeolite

JACQUES C. VÉDRINE,*,[1] ALINE AUROUX,* VERA BOLIS,*,[2] PIERRE DEJAIFVE,*,[3]
CLAUDE NACCACHE,* PIOTR WIERZCHOWSKI,*,[4]
ERIC G. DEROUANE,† JANOS B. NAGY,† JEAN-PIERRE GILSON†
JAN H. C. VAN HOOFF,‡ JAN P. VAN DEN BERG,‡ AND JILLUS WOLTHUIZEN‡

* *Institut de Recherches sur la Catalyse, C.N.R.S., 79, Boulevard du 11 Novembre 1918, F-69626-Villeurbanne Cédex, France;* † *Facultés Universitaires de Namur, Laboratoire de Catalyse, Rue de Bruxelles, 61, B-5000-Namur, Belgium; and* ‡ *Technische Hogeschool Eindhoven, Laboratorium voor Anorganische Chemie, P.O. Box 513, NL-Eindhoven, The Netherlands*

Received September 11, 1978; revised February 9, 1979

The infrared spectra of the H–ZSM-5 zeolite calcined at temperatures up to 1173 K, and the corresponding electron spin resonance and microcalorimetric data are discussed. Two types of hydroxyl groups are characterized by absorption bands at 3720 and 3605 cm^{-1}, a small shoulder being present at 3665 cm^{-1}. Infrared spectra were also recorded after pyridine adsorption, showing the presence of Brønsted acid sites and Lewis acid sites. After calcination at increasing temperatures, dehydroxylation of the zeolite is observed: above 675 K, the number of Brønsted acid sites decreases, while that of strong Lewis acid sites increases; however, a small dealumination occurs as shown by chemical analysis measurements and XPS data. Moreover, dehydroxylation enhances the constraint character of this zeolite, as observed by pyridine inability to titrate the total Lewis sites. Electron spin resonance studies of trapped hydrogen atoms, of adsorbed NO, and of adsorbed benzene radical cations formed on H–ZSM-5 at various calcination temperatures are discussed in terms of the number and strength of the acid sites. It is suggested that the acid sites which are present are very similar to those of H–mordenite although slightly stronger. A microcalorimetric study of ammonia adsorption confirms the very strong acidic character of the acid sites and shows their dependence in strength and heterogeneity upon calcination temperature.

INTRODUCTION

Extensive research has been reported on the relationship existing between the acidity of zeolites and their catalytic properties. Recently a new type of zeolite, so-called "ZSM," synthesized by Mobil, has shown interesting properties for the conversion of methanol and other compounds to higher hydrocarbons (*1*, *2*). The mechanism reported by us (*2*) suggested that an

---

[1] To whom queries concerning this paper should be sent.

[2] Postdoctoral fellow 1977–1978. Permanent address: Istituto di Chimica Generale e Inorganica, Facoltà di Farmacia, Università di Torino, Torino, Italy.

[3] Postdoctoral fellow 1977–1979. Permanent address: Facultés Universitaires de Namur, Laboratoire de Catalyse, B-5000-Namur, Belgium.

[4] Postdoctoral fellow 1977–1978. Permanent address: Instytut Chemii Organicznej Polskiej Akademii Nauk, ul. Kasprzaka 44, 01-244 Warszawa, Poland.

0021-9517/79/110248-15$02.00/0

TABLE 1

Chemical Analysis of ZSM Samples Prepared at Two Different Al Contents[a]

	H_2O calcined at 1100°C (wt%)	Al_2O_3 (wt%)	Na_2O (wt%)	SiO_2 (wt%)	Chemical formulas
H–ZSM$_1$	4.15	4.25	0.03	95.72	$Si_{91,25}Al_{4,75}Na_{0,06}H_{4,69}O_{192}$, $13H_2O$
Na–ZSM$_1$	4.45	4.21	0.73	95.06	$Si_{91,25}Al_{4,75}Na_{1,43}H_{3,32}O_{192}$, $14.3H_2O$
Na–ZSM$_2$	11.0	0.96	0.13	98.91	$Si_{94,8}Al_{1,2}Na_{0,25}H_1O_{192}$, $35.2H_2O$

[a] Results are given in weight percent for fully hydrated materials, and the chemical formulas are calculated taking 96 (Si + Al) atoms per unit cell as in Ref. (*4*).

intermediate formed by dehydration of methanol was rapidly converted by proton addition into a carbenium ion which underwent polymerization and cyclization in contrast to the carbene mechanism proposed by Chang and Silvestri (*1*). Catalysis by acidic sites was thus proposed. However, up to now, no data on the acidic properties of this material were available. Thus, it appeared important to us to investigate the acidic properties of the ZSM-5 zeolite as knowledge of the surface chemistry of these materials could shed light on the nature of the active sites.

This paper reports an infrared study of the structural hydroxyl groups as a function of dehydration temperature. Pyridine adsorption allowed the characterization of Brønsted and Lewis acid sites. The electron acceptor properties were followed by investigating the ESR spectra of adsorbed electron donor molecules. Furthermore, the strength of acid sites was estimated by measuring the heat of ammonia adsorption.

EXPERIMENTAL

The ZSM-5 type zeolites were synthesized following the procedure previously described (*2*, *3*). HCl treatment at 353 K of the sodium form resulted in the formation of the H-form. Our samples are denoted as X–ZSM$_y$, X being Na or H (sodium or protonated form), y referring to the preparation batch. Chemical compositions of the various samples are given in Table 1. Note that the so-called Na–ZSM$_2$ sample was prepared without adding sodium aluminate to the silica dissolved in aqueous solution of tetrapropylammonium hydroxide. Indeed, the Al and Na contents (see Table 1) arose from sodium attack on the Pyrex container at 423 K. A pure crystalline silica ($Al < 0.06$ wt%) (or silicalite (*5*)) was obtained using a Teflon-walled metallic container but was not studied in the present work. X ray diffraction patterns were in agreement for all samples with those reported by Argauer and Landolt (*3*) and showed that the samples were well crystallized without any detectable amorphous phase. Electron micrographs using a JEOL JEM 100 CX transmission electron microscope and scanning electron micrographs obtained with a JEOL JSM 35 instrument showed that the material was composed of platelets, with sizes ranging from 0.1 to 0.5 μm (thickness) and 1 to 5 μm (other two dimensions) as shown in Fig. 1, and of much smaller particles ($\phi = 0.1$ μm) without a particular shape.

Infrared measurements were performed on a Perkin–Elmer 125 spectrometer. The spectral region between 4000 and 1300 cm^{-1} was examined. Thin wafers of zeolite (6 mg/cm^{-2}) formed by pressing the zeolite powder were mounted on a quartz sample holder and introduced into a special infrared cell described elsewhere (*6*). The ir cell allowed the thermal treatment *in vacuo*

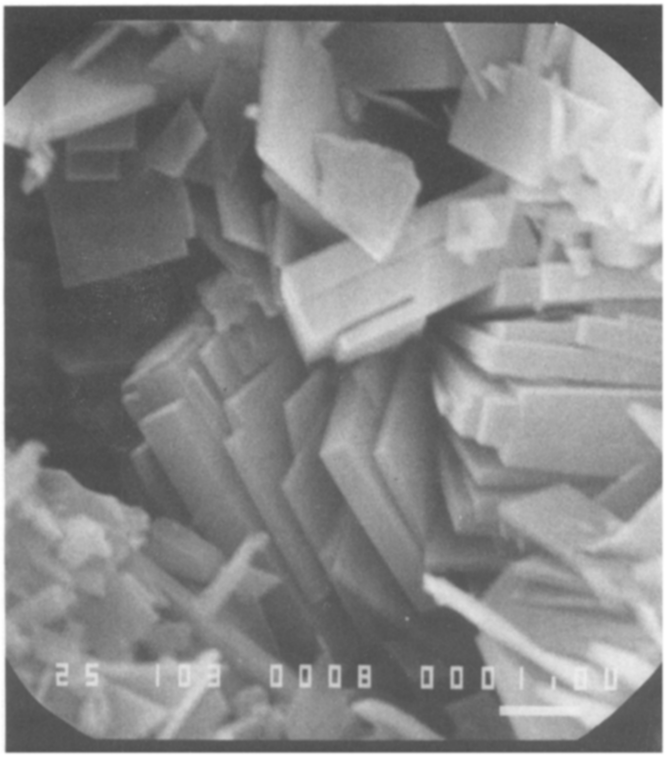

FIG. 1. Scanning electron micrographs for H–ZSM$_1$ sample showing platelets. The white horizontal mark corresponds to 1 μm.

of the samples up to 1200 K and pyridine adsorption experiments. Pyridine vapor, dehydrated before use, was adsorbed at room temperature on the activated wafer and then outgassed at various temperatures with subsequent recording of the ir spectra.

ESR spectra were recorded with an E9 X-band Varian spectrometer using 100-kHz field modulation. Absolute measurements of the number of spins per gram of sample were made by using diphenyl-picryl hydrazyl(DPPH) as standard. For ESR studies the samples were placed in an ESR silica tube and degassed at various temperatures. Hydrogen atoms were generated by γ irradiation of the samples at doses of about 1 Mrad at 78 K and were studied by ESR (*7*).

For the ESR study of NO adsorption, NO was contacted at 298 K with the activated zeolite sample and then cooled slowly to 78 K, before recording the ESR spectra at that temperature (*8*).

An identical procedure was chosen for the ESR study of adsorbed benzene. However, all ESR spectra were recorded at 298 K. Furthermore the degassed samples were, before benzene adsorption, contacted with dry oxygen at the temperature chosen for the dehydration and then the oxygen in excess was removed by pumping. This activation procedure is known to enhance the formation of radical cations (*8*, *9*).

Calorimetric studies of NH_3 adsorption were performed using a Tian–Calvet calorimeter and allowing the adsorption of small increments of NH_3 on samples activated *in vacuo* at different temperatures. About 100 mg of sample were used, and NH_3 increments were of 90 μmol/g of catalyst.

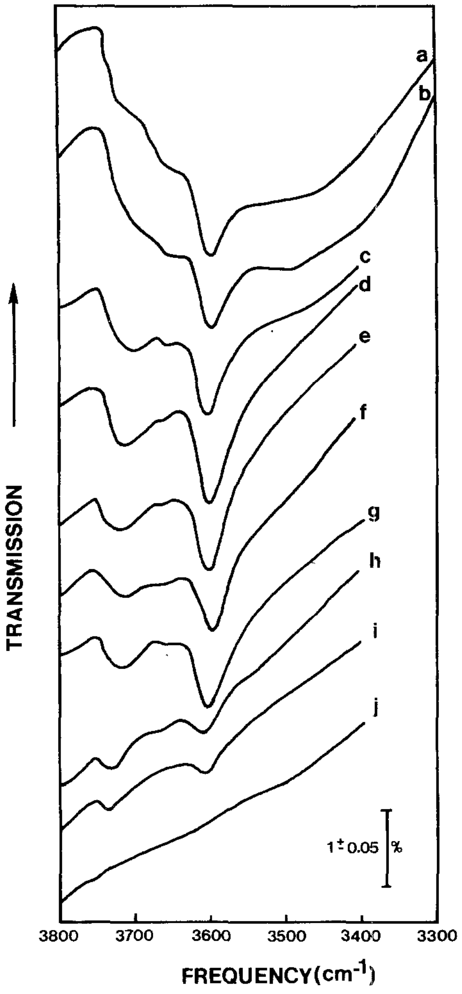

FIG. 2. Infrared absorption bands of OH groups of the H-ZSM$_1$ zeolite heated *in vacuo* (10^{-5} Torr) at different temperatures. (a) 298 K, (b) 373 K, (c) 573 K, (d) 673 K, (e) 737 K, (f) 755 K, (g) 773 K, (h) 963 K, (i) 1063 K, (j) 1163 K.

XPS measurements were performed using a Vacuum Generators VG-III spectrometer. The samples were first heated outside the spectrometer *in vacuo* in the temperature range, 773–1173 K, cooled down to room temperature, and then contacted with air. They were then introduced into the spectrometer and evacuated to 10^{-9} to 10^{-10} Torr at 298 K. The spectrometer was controlled by computer and allowed us to accumulate Al spectra for 10 hr. Binding energies and intensities were analyzed by computer.

EXPERIMENTAL RESULTS

Infrared study of structural hydroxyl groups. The infrared spectra of H-ZSM$_1$ samples dehydrated *in vacuo* between room temperature and 1200 K are shown in Fig. 2. The sample outgassed at 298 K showed a broad ir band in the 3800- to 3400-cm^{-1} region in which peaks at 3720 and 3605 cm^{-1} and a shoulder at 3665 cm^{-1} were clearly observed. Furthermore a band at 1630–1640 cm^{-1} was also present. The latter is due to overlap between the band assigned to the Si–O stretching mode and the H_2O bending mode of physically adsorbed water. Upon dehydration of the wafer up to 773 K, the intensity of this band decreases only slightly, indicating that the amount of physically adsorbed water on the zeolite is low. These ir results are in agreement with the quantitative measurement of weight loss when the sample is calcined between 300 and 1200 K. The weight loss found less than 5 wt% in the case of H-ZSM$_1$ zeolite (Table 1) while, in general, the same parameter for faujasite-type zeolite is greater than 25 wt% in the same temperature range. The ir spectra of H-ZSM$_1$ dehydrated above 473–573 K showed two well-resolved ir bands, at 3720 and 3605 cm^{-1}, respectively, and a shoulder at 3665 cm^{-1}. Figure 3 shows the variations of the intensities of these ir bands as a function of the calcination temperature. The ir bands intensity remained constant in the first stage of calcination. Above 673 K dehydroxylation occurred with a subsequent decrease of the absorption bands in the hydroxyl stretching region. The dehydroxylation was essentially complete at 1173 K. The infrared results for a sample heated *in vacuo* at 1173 K and subsequently rehydrated at room temperature under 18 Torr of water vapor showed that only the bands at 3720 and 1640 cm^{-1} were restored.

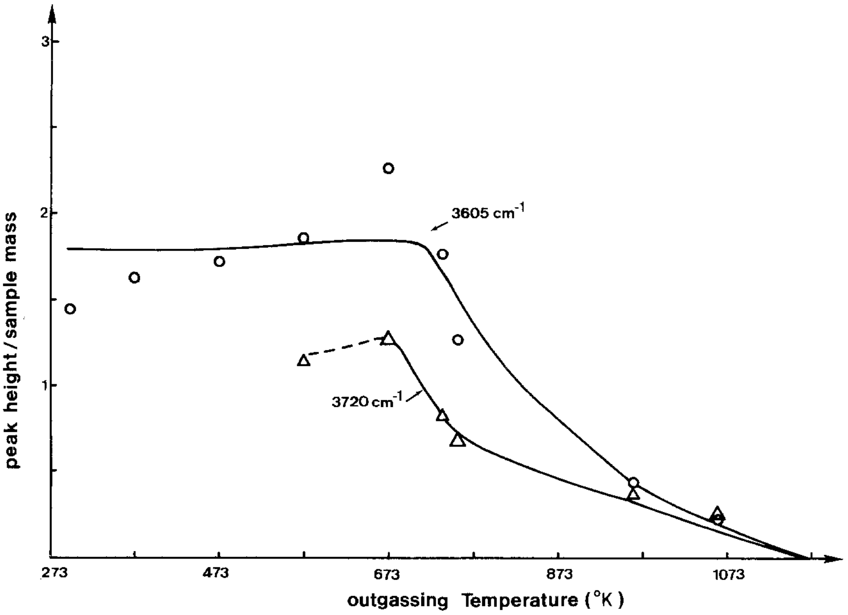

FIG. 3. Variation of ir-band height of hydroxyl groups versus H–ZSM$_1$ outgassing temperature. (○) 3605-cm^{-1} band, (△) 3720-cm^{-1} band.

Pyridine adsorption (*ir*). Infrared spectra of pyridine adsorbed on acid catalysts have often been used for characterizing the nature and strength of acid sites (*10*). Such experiments were performed on an H–ZSM$_1$ sample calcined at various temperatures. Figure 4 shows typical ir spectra for chemisorbed pyridine. After adsorption of pyridine at room temperature and further outgassing at 423 K to release physisorbed pyridine, absorption bands due to chemisorbed pyridine were observed at 1645, 1628, 1550, 1495, and 1460 to 1450 cm^{-1}. Simultaneously, the hydroxyl stretching bands at 3720, 3665, and 3605 cm^{-1} disappeared almost completely. Absorption bands at 1550 and 1460 to 1450 cm^{-1} indicate the presence of both Brønsted and Lewis acid sites (*10*). Figure 5 represents the variations of the 1550- and 1460- to 1450-cm^{-1} band intensities as a function of the dehydration temperature. The data shown in Fig. 5 indicates that the band at 1550 cm^{-1}, attributed to pyridinium ions, followed the same trend as that found for the hydroxyl stretching band at 3605 cm^{-1}, confirming that above 775 K the Brønsted acidity decreases as the dehydration temperature increases. Furthermore, by contrast to the behavior of the H-form of Y zeolite, a simultaneous decrease in the ir band at 1460–1450 cm^{-1} is observed.

The acid strength of the hydroxyl groups was estimated by following the restoration of the hydroxyl bands upon desorbing pyridine *in vacuo* at increasing temperatures. The results show that the ir band at 3720 cm^{-1} is first restored, while the band at 3605 cm^{-1} is recovered only after degassing at about 673 K. These data indicate that the OH groups responsible for the ir band at 3605 cm^{-1} are the most acidic although the acidic character of the hydroxyl groups showing the ir band at 3720 cm^{-1} was further proved by the following experiment.

An H–ZSM$_1$ sample dehydroxylated at 1173 K and then rehydrated at 298 K (equilibration with 18 Torr of water) showed, after degassing the excess water, an ir band at 3720 cm^{-1} (as stated above).

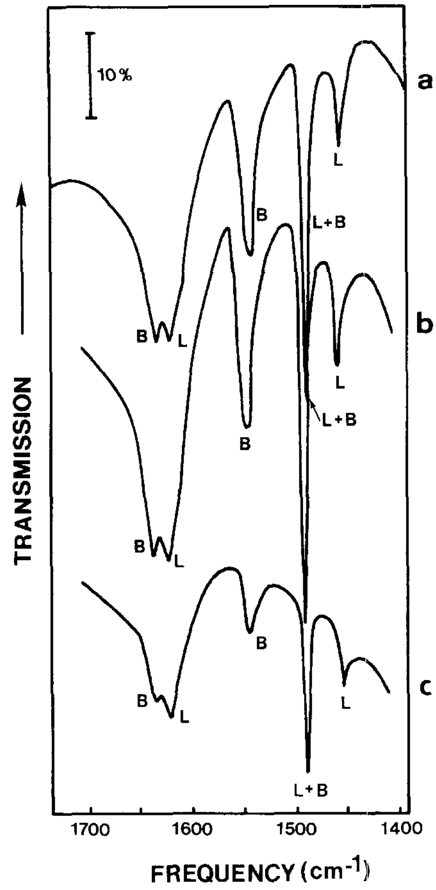

Fig. 4. Typical ir bands in the 1700- to 1500-cm^{-1} region for pyridine adsorbed at room temperature and outgassed at 423 K for H-ZSM$_1$ sample. Outgassing temperatures: (a) 573, (b) 755, (c) 963 K. B, Brønsted sites; L, Lewis sites.

Upon pyridine adsorption at room temperature and outgassing at 423 K this band was removed and ir bands at 1640, 1550, and 1495 cm^{-1} due to pyridinium species appeared.

It is interesting to note that the band at 3720 cm^{-1} is broad which could indicate either an overlap of several ir bands due to the presence of nearly equivalent OH groups or an interaction of OH groups with water molecules to form $(H_2O)_nH^+$-like species (*11*). Furthermore the H-ZSM$_2$ sample, having a lower aluminum content, showed only the ir band at 3720 cm^{-1}. The corresponding OH groups also reacted with pyridine to form the pyridine ion.

Atomic hydrogen species (*ESR*). As shown previously (*7*), γ irradiation releases hydrogen atoms characteristic of the hydroxyl groups in the zeolite lattice. Similar H-ZSM$_1$ samples, which were irradiated by γ rays at 78 K, exhibit an ESR spectrum characteristic of hydrogen atoms trapped within the zeolite framework. The ESR spectrum of H atoms trapped in the H-ZSM$_1$ zeolite is due to the overlap of two components. One is narrow with a first-derivative peak-to-peak width, ΔH_{pp}, equal to 1.1 ± 0.05 G, a hyperfine splitting, A, of 507.8 ± 0.2 G and a g-factor, g, of 2.0024 ± 0.001, and the other is "broad" with $\Delta H_{pp} \simeq 2.2 \pm 0.2$ G, $A = 503.5 \pm 0.5$ G, and $g = 2.0024 \pm 0.0001$. Quantitative measurements of the amount of H atoms trapped at 78 K are given in Fig. 6.

The number of trapped H atoms corresponding to the narrow ESR line varies in the same manner as the OH groups corresponding to the 3605-cm^{-1} ir band while the broad ESR line parallels the 3720-cm^{-1} band. Close behavior of this type was also observed for an H-Y zeolite (*12*) although the thermal stability of the trapped H atoms was better (recombination above 150 K) for the H-ZSM sample than for the H-Y zeolite (disappearance above 100 K). The hyperfine splitting was also larger than for the H-Y zeolite: 507.8 against 501.8 G for the narrow line (1.1 against 1.25 G in width) and 503.5 against 499.8 G for the broad line (2.2 against 3.6 G in width). According to Adrian (*13*), the increase in the hyperfine splitting could be due to increased Pauli exclusion forces or to a change in unpaired electron density due to a weak charge transfer bond between H atoms and lattice atoms. In any case, these results show that trapping sites and trapping strength for H atoms are different for both types of zeolite. The main feature is, however, that variations in the number of trapped H atoms as a function of dehydration conditions follow that of the ir band intensities for the acidic OH groups. As the width of an ESR line of trapped H atoms is mainly governed by dipolar interaction, presumably with protons from nearby water molecules as suggested by Iton and Turkevich (*14*), it is tempting to suggest in addition that the OH groups giving rise to the 3720-cm^{-1} ir band and the broad ESR line are surrounded by water molecules while the other OH groups are not.

NO adsorption (*ESR*). The ESR signal of NO adsorbed on calcined H–ZSM_1 zeolite ($g_\perp = 1.995$ and $g_{\parallel} \simeq 1.954$) is similar to that already observed on decationed faujasite and on acidic mordenite (*8*). The ESR spectrum shows a hyperfine structure attributed to the interaction of the unpaired electron with an aluminium nucleus (and a hyperfine splitting of roughly 13 G (*15*)). Thus, it is clear that NO is adsorbed on or near an aluminium atom. Such an ESR signal characterizes strong Lewis sites (*8*), which allows one to follow the formation of such sites as a function of dehydration conditions. The dependence of the NO spin concentration as a function of the dehydration temperature of the zeolite is plotted in Fig. 7. The most striking feature is the sharp increase in the ESR intensity above 773 K.

Benzene radical formation (*ESR*). The adsorption of perylene, anthracene, and naphthalene on H–ZSM_1 zeolite heated up to 1073 K did not show the formation of the corresponding radical cation. However, although benzene has a much higher ionization potential, a well-resolved ESR spectrum with seven hyperfine lines split by ca. 4.4 G appeared when its vapor was contacted with H–ZSM_1 zeolite. This spectrum was formerly identified as that of the benzene radical cation (*16*) formed by electron transfer between benzene and electron acceptor sites.

Pretreatment with dry oxygen at the dehydration temperature before benzene adsorption was found to enhance the formation of the radical species. Figure 8

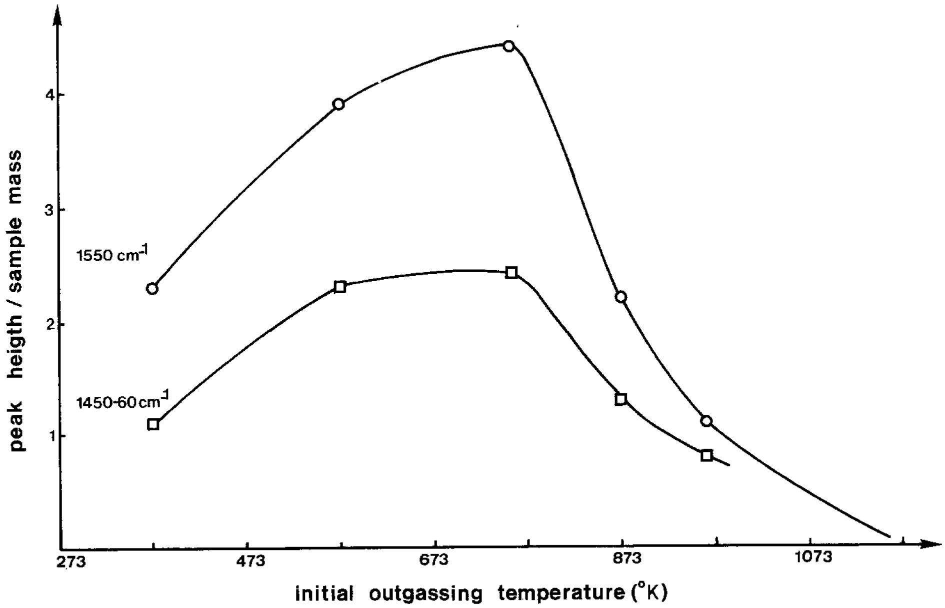

FIG. 5. Variations of 1550- and 1450- to 1460-cm^{-1} ir band intensity as a function of outgassing temperature of H–ZSM_1 sample.

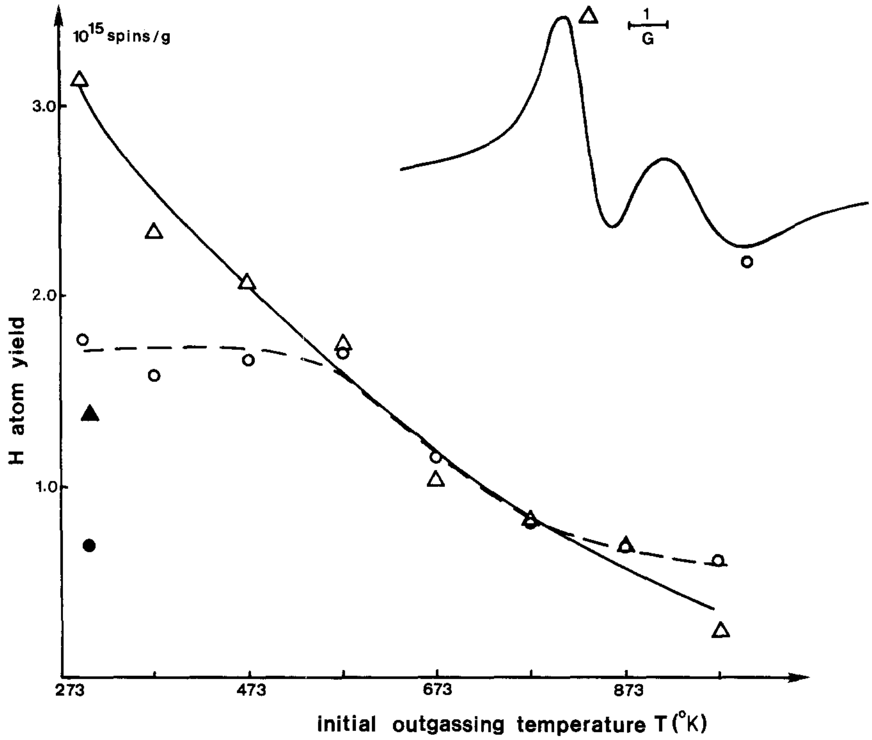

FIG. 6. H atom yield as a function of initial outgassing of H-ZSM$_1$ zeolite temperature. The samples were γ-irradiated at 78 K. Only the low field lines at ca-3050 g given for samples outgassed at 473 K. (△) Narrow ESR line, (○) Broad ESR line, (▲) Na-ZSM zeolite narrow line, (●) Na-ZSM zeolite broad line.

gives the benzene cation concentration variation versus the activation temperature for two different activation treatments. It is seen that the number of electron acceptor sites increases with the dehydration temperature, particularly when dehydroxylation occurs above 775 K. The fact that benzene cations were formed while perylene or anthracene molecules with lower ionization potential values, but larger steric diameter, were not ionized, indicates that the strong Lewis acid sites of the zeolite are located inside the structural channels having ellipsoidal openings (5.1–5.7 Å) (*5*).

XPS data. Typical XPS results for H-ZSM$_1$ are presented in Table 2, the binding energy values being arbitrarily referred to the O 1s line at 532.4 eV as was done for type Y-zeolites (*17*). The intensities (*I*) of the XPS lines were converted into element concentration ratios using the classical relationship:

$$\frac{n_1}{n_2} = \frac{I_1}{I_2} \cdot \frac{\sigma_2 (E_{k_2})^{\frac{1}{2}}}{\sigma_1 (E_{k_1})^{\frac{1}{2}}},$$

where σ and E_k correspond to the electron cross section given by Scofield (*18*) and to the kinetic energy value, respectively. The main feature of these XPS results is the small but significant increase of roughly 20% in the Al/Si ratio as the outgassing temperature increases from 773 to 1173 K. Note that the corresponding value for the hydrated material, as calculated from the chemical analysis data, is 0.026.

Calorimetric study. Determination of the NH$_3$ chemisorption heat was performed to characterize the acid strength of the zeolite and to have an idea of their distribution in strength. Small increments of NH_3 were successively added to the samples maintained at 416 K in the calorimeter. The variations in the heat of adsorption as a function of increasing NH_3 coverage, for different initial outgassing temperatures, are shown in Fig. 9. Two main features are noticed. First, the chemisorption energy value decreases with the amount of NH_3 introduced; this characterizes the acid strength heterogeneity. Second, the heterogeneity range and the initial chemisorption energy greatly depend on the outgassing temperature. It follows that high activation temperatures decrease the total number of acid sites although some of them have an enhanced acid strength.

It is worthwhile at this stage to compare the absolute number of acid sites measured by microcalorimetry to the number of potential acid sites estimated from the chemical formula of the zeolite (Table 1). About 4.7 Brønsted sites per unit cell may exist at maximum, resulting in 2.35 Lewis sites after dehydroxylation. The curves of Fig. 9 indicate that about 3.2, 3.1, and 2.5 sites are detected by microcalorimetry for samples activated at 743, 923, and 1073 K, respectively. Therefore, part of the Brønsted sites are too weakly acidic to be detected, in the NH_3 range pressure used, because of reversible adsorption (with a heat of adsorption of about 63 kJ mol^{-1}). Note that for physisorbed NH_3, the adsorption heat is roughly 25 kJ mol^{-1}.

Thermal stability. The structural stability of H-ZSM-5 sample as a function of thermal treatment *in vacuo* was studied. The X-ray diffraction patterns were unchanged when the sample was outgassed up to 1200 K.

H-ZSM_I-5 samples outgassed at 773 and 1200 K were treated in a HCl, N/2

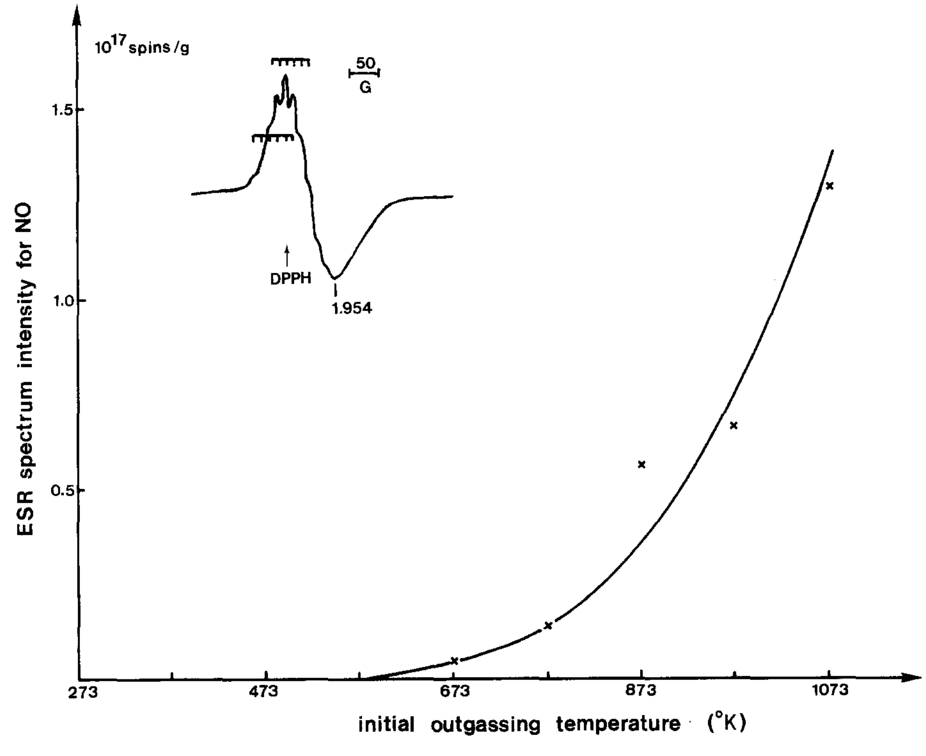

FIG. 7. Variations of ESR spectrum intensities of NO adsorbed of H–ZSM_I zeolite as a function of initial outgassing temperature.

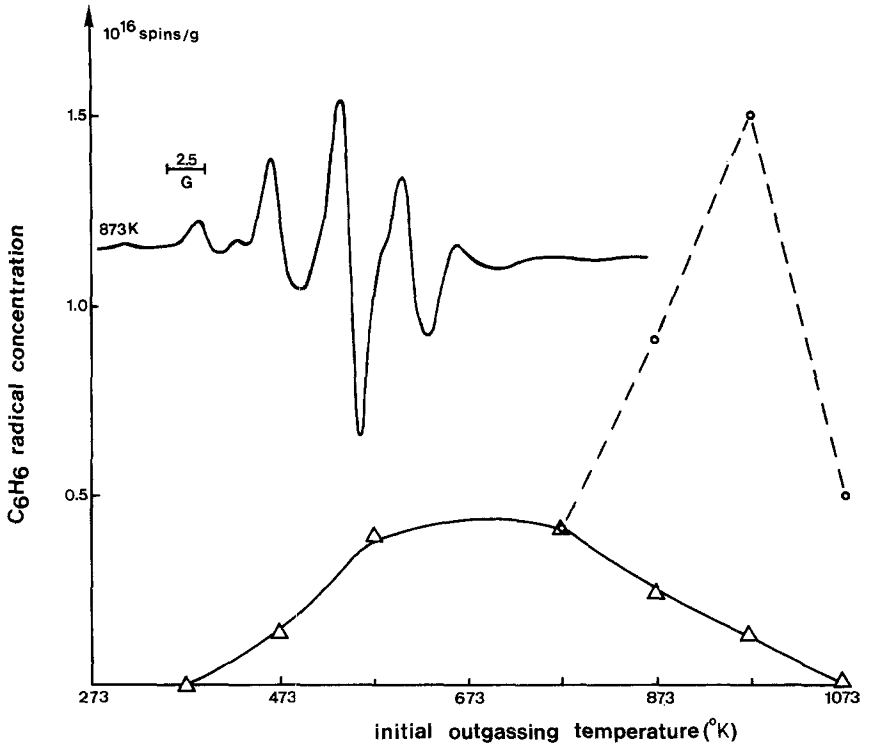

FIG. 8. Variations of ESR spectrum intensity of $C_6H_6^+$ adsorbed of H-ZSM$_1$ zeolite as a function of initial outgassing temperature. (△) Heated under O_2 and then outgassed at the same temperature; (○) heated under O_2 at the temperature indicated and then outgassed at 773 K.

solution at room temperature and then subjected to chemical analysis. The hydrochloric acid treatment was performed to dissolve any nonstructural aluminium compound which might be removed from the zeolite lattice by the heat treatment as was observed in the case of H-Y zeolite, mainly in deep bed conditions (*19*, *20*). The results showed that the aluminium content of HCl-treated samples after outgassing at 1200 K has decreased by about 15% with respect to the 773 K sample. This result was in agreement with XPS data, and one can suggest that a small dealumination occurred during the dehydroxylation at high temperature.

TABLE 2

XPS Data for H-ZSM$_1$ Zeolite Outgassed at 773 or 1173 K[a]

Heat treatment temperature (K)	O 1s		Si 2s		Si 2p		Al 2p		O/Si	Al/Si
	E_b	$\Delta E_{\frac{1}{2}}$	E_b	$\Delta E_{\frac{1}{2}}$	E_b	$\Delta E_{\frac{1}{2}}$	E_b	$\Delta E_{\frac{1}{2}}$		
773	532.4	2.4	154.0	3.0	103.0	2.4	74.7	2.7	2.6	0.043
1173	532.4	2.4	154.0	3.0	103.0	2.3	74.5	2.5	2.55	0.054

[a] The O/Si and Al/Si ratios are deduced from line intensity ratios as mentioned in the text. Binding energy (E_b) and total linewidth at half height ($\Delta E_{\frac{1}{2}}$) are expressed in eV. Accuracy estimated as ±0.2 eV.

DISCUSSION AND CONCLUSIONS

Infrared spectroscopy of structurally different zeolites in their hydrogen form has been the subject of numerous investigations (*21*). Synthetic X and Y zeolites in their H-form have hydroxyl bands at about 3740, 3640, and 3540 cm^{-1} while mordenite shows hydroxyl bands near 3740 and 3600 cm^{-1} (*22*). It was generally agreed that the band at 3740 cm^{-1} represents Si–OH groups either terminating the zeolite lattice or present on residual amorphous silica as impurity. These OH groups showed nonacidic properties as they interacted with a base such as pyridine only by hydrogen bonding. However, our experimental data on a ZSM-5-type zeolite show that the highest frequency, in the OH stretching region, is 3720 cm^{-1}. The band at 3720 cm^{-1} is probably generated by OH groups attached to silicon since the band intensity does not vary significantly when the ratio Si/Al is increased (H–ZSM_1 and H–ZSM_2 samples). Furthermore, the ν(OH) shift to lower frequencies could indicate that the OH responsible for the ir band at 3720 cm^{-1} has its proton less strongly bound and therefore has a weak acidic character. Pyridine adsorption results have confirmed this suggestion.

It was also observed that the 3720-cm^{-1} bandwidth was strongly dependent on the outgassing temperature. If we assume that the bandwidth reflects the degree of interaction of the OH with water molecules, then the band at 3720 cm^{-1} may be attributed to $H^+(H_2O)_x$ groups (*11*), water molecules being almost completely removed at about 573 K. Chen (*23*) has suggested that the specific interaction between water molecules and the protons in mordenite with SiO_2/Al_2O_3 ratio above 10 corresponds

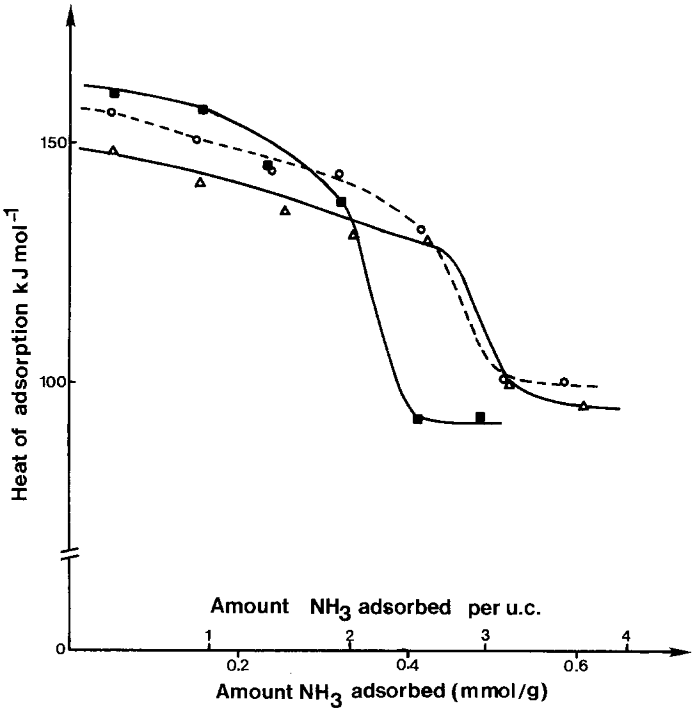

FIG. 9. Variation of heat of adsorption of NH_3 as a function of NH_3 increments. The calorimeter was maintained at 416 K. The H–ZSM_1 sample was initially outgassed at 743 (Δ), 923 (○), and 1073 K (■).

to about four H_2O molecules around each H^+ forming a hydroxonium $(H_9O_4)^+$-like structure. By analogy with H–mordenite we could suggest that similar hydroxonium species are present on slightly dehydrated H–ZSM-5 samples.

Karge (*22*) and Eberly *et al.* (*24*) have reported a hydroxyl stretching at 3610 and 3590 cm^{-1}, respectively, for H–mordenite. In our study an absorption band at 3605 cm^{-1} was also found.

It was observed that the OH group concentration varied only slightly as the outgassing temperature was increased up to about 675 K. Above this temperature a sharp decrease of the OH group concentration occurred, and at about 1200 K the H–ZSM-5 sample appeared to be completely dehydroxylated. The similarity in the behavior of H–mordenite and H–ZSM-5 zeolites is also found when comparing the change of the two OH ir band intensities (Fig. 3) following degassing of the sample at increasing temperature with the data of Karge (*22*).

The ESR studies of hydrogen atoms formed by γ irradiation provide additional data in favor of our suggestion of two different hydroxyl groups as observed by ir. As mentioned above it is possible in principle to deduce the state of hydration of the surface by analyzing the linewidth of the hydrogen atom ESR signal (*14*). Since the ESR spectra of H atoms stabilized on the H–ZSM-5 zeolite are formed by two signals having different linewidths, it is obvious that hydrogen atoms are stabilized in at least two different environments. The broad ESR signal is probably generated by hydrogen atoms strongly interacting with other protons (strong dipolar interaction). Furthermore the intensity of the broad ESR signal of $H^{\cdot}$ varies as the intensity of the 3720-cm^{-1} infrared band. Hence, these results tend to support our conclusion that the OH groups responsible for the ir band at 3720 cm^{-1} are involved in the formation of the broad H° atom ESR signal. The assignment of the broad ESR signal to hydrogen atoms interacting with nearby protons, and the identification of the source of these hydrogen atoms as the hydroxyl groups responsible for the ir band at 3720 cm^{-1}, provide additional evidence for the existence of $(H_2O)_xH^+$ centers in the H–ZSM-5 zeolites.

It is generally assumed that upon dehydroxylation conversion of Brønsted acid sites to Lewis acid sites occurs and that the tricoordinated aluminium ions formed by calcination at elevated temperatures are reconverted into Brønsted acid sites upon rehydration at room temperature. In marked contrast, the 3605-cm^{-1} band was not regenerated by rehydration of the H–ZSM-5 zeolite calcined at 1173 K. Since X-ray diffraction analysis has indicated that the crystallinity of the zeolite was maintained after the high-temperature treatment, one could conclude that in the H–ZSM-5 type zeolite, Lewis acid sites cannot be rehydrated into Brønsted acid sites. Thus, assuming that the 3605-cm^{-1} band is due to Si–OH–Al groups as in faujasite or mordenite zeolites, the total and irreversible disappearance of the band at 1173 K could indicate that under calcination at elevated temperature, some aluminium ions are removed from the zeolite lattice and may then impede hydration of the internal Lewis sites.

The existence of at least two distinct types of hydroxyl groups has been provided by our ir studies. Evidence for the acidic character of these groups was obtained from pyridine adsorption since pyridinium ions were observed by reaction with hydroxyl groups. However, in contrast with the H–Y zeolite, our infrared results have shown that both the bands at 1540 (Brønsted acidity) and at 1450–1460 cm^{-1} (Lewis acitidy) decreased with increasing calcination temperature, which would indicate that both Brønsted and Lewis acidities decreased. Cannings (*25*) has also observed an overall decrease in acidity of H–mordenite upon calcination at elevated temperature and interpreted these findings as structural changes of mordenite. The experimental decrease of the number of pyridine molecules coordinated to Lewis acid sites may be due to a dealumination of the sample and/or to a decrease of the Lewis sites accessibility through the zeolite channels. Such a limited accessibility of pyridine to zeolite channels has previously been observed by Ben Taarit (*26*) on H–mordenite samples. The calorimetric measurements have provided more quantitative information concerning the strength and the number of acid sites. The initial heats of adsorption of ammonia were stronger (150–163 kJ mol^{-1} NH_3) than those measured on other zeolites (113–117 kJ mol^{-1} NH_3) (*27*, *28*). These strong acid sites may afford a pathway for carbenium ion polymerization, hydrogen transfer, and cyclization reactions as proposed for the conversion of methanol (*2*). Note also that steric hindrance of molecules to enter zeolite channels was demonstrated by a detailed analysis of calorimetric data for NH_3 adsorption (*29*).

It was noted in the course of the above discussion that in many instances both H–mordenite and H–ZSM-5 zeolites showed similar acidic properties. The picture obtained from the ESR study of electron donor molecules adsorbed on the surface of H–ZSM-5 reinforces these ideas and provides additional information on the shape and accessibility of the active sites. There is a wide agreement that the formation of radical cations from aromatic compounds on acidic materials proceeds via a one-electron transfer from the aromatic compound to a Lewis acid site, with the need for an aromatic molecule with a low ionization potential (IP) and/or a Lewis acid site with a high electron affinity (*30*). Since benzene cation radical was formed on adsorbing C_6H_6 (IP = 9 eV), this study proved that H–ZSM-5 zeolite, like H–mordenite, has strong electron acceptor properties. Furthermore, as for mordenite, the presence of adsorbed oxygen considerably enhanced the oxidizing properties (*9*). of the H–ZSM zeolite. It is then clear that the sites responsible for the electron transfer are identical on both zeolites.

It was also shown previously (*9*, *32*) that when benzene was adsorbed on mordenite the monomeric benzene radical was first generated and further transformed into a dimeric benzene radical, leading ultimately to the biphenyl cation radical. This indicates that the void space of the mordenite channels was large enough to accommodate a benzene cation radical dimer in a sandwich form. In contrast our experimental results have shown that the ESR spectrum of adsorbed benzene was characteristic (Fig. 8) of the monomeric cation radical of benzene (*16*). It is thus clear that the channels of the H–ZSM-5 zeolite cannot accommodate a sandwich-like structure such as the dimeric benzene radical, and this explains why it has not been possible to form anthracene or naphthalene cation radicals whereas these radicals were stabilized on H–mordenite (*26*). This is an example of the pore-size effect in molecular sieving.

The ESR results of NO adsorbed on the H–ZSM-5 sample shown in Fig. 7 indicate that the number of sites responsible for the NO adsorption in its paramagnetic form, which were identified to strong Lewis sites (*31*), increases with the temperature of dehydroxylation. It must be noticed that the adsorption of NO in its paramagnetic form, giving thus an ESR signal, concerns only the Lewis acid sites having high electron acceptor properties, i.e., the very strong Lewis acid sites. Hence, increasing the acid strength will be more important for NO adsorption than increasing or decreasing the number of total Lewis sites. The increase of the number of trigonal aluminium revealed by NO adsorption is in accord with the suggestion that pyridine, due to its size, is unable to reveal all the trigonal aluminium ions present in the H–ZSM channels.

Another interesting feature of the H–ZSM-5 zeolite is its low water content. In general zeolites are highly hydrophilic and they adsorb a large amount of water. Recently, however, Chen (*23*) showed that the hydrophilic properties of mordenite were decreased by aluminium removal (a dealuminated mordenite with SiO_2/Al_2O_3 ratio higher than 80 was almost completely hydrophobic), and Flanigen *et al.* (*5*) synthesized a new silica molecular sieve which was hydrophobic. These recent reports suggest that the effect of decreasing the amount of aluminium in molecular sieves is to render them hydrophobic. H–ZSM-5 zeolites, even when only outgassed at room temperature, show a small ir band at 1640 cm^{-1}. Since the intensity of the 1640-cm^{-1} band can be used as an indication of the amount of adsorbed water on zeolite, the low intensity of this band indicates that the H–ZSM-5 zeolites show a low affinity for water, in agreement with their high Si/Al ratio. The hydrophobic character of the H–ZSM-5 zeolite may, of course, play an important role in the methanol conversion, since the adsorption of the water formed during the methanol conversion would then not compete dramatically with hydrocarbon reactions.

In conclusion, this work has shown that the hydrogen form of the ZSM-5 zeolite contains acidic hydroxyl groups similar to those existing on H–mordenite. The acid strength of H–ZSM-5 is slightly higher than that of acidic mordenite, the two zeolites differing mainly by the number of acid sites. Thus one would expect that the two solids would behave similarly for reactions catalyzed by acids. However, in this work, it has been shown that the pore size of H–ZSM-5 prevents the formation of a dimeric benzene radical as well as the diffusion of naphthalene molecules through the zeolite lattice whereas mordenite allows both. Thus a small difference in pore size of less than 1 Å strongly modifies the adsorption of molecules, and then affects their reactivity and selectivity in hydrocarbon conversion.

This work has also provided evidence that small dealumination and accessibility hindrance occur by calcination of the H–ZSM-5 zeolite at elevated temperature; the dehydration at high temperature irreversibly removes the more acidic hydroxyl groups. It might thus be interesting to investigate the effect of the activation temperature of the H–ZSM zeolite on its activity and/or selectivity for methanol conversion.

The hydrophobic character observed for dealuminated H–mordenite is also found for the H–ZSM-5 zeolite, the adsorption of water molecules depending on the number of acidic silanol groups.

ACKNOWLEDGMENTS

This work was partly sponsored by CNRS (France) under grant ATP Internationale No. A 651-3196. The authors thank Dr. M. Bartholin for electron scanning micrographs, C. Leclercq and I. Mutin for electron micrographs, the Centre Commun ESCA of the University of Lyon for the use of the VG-III spectrometer, and the analytical laboratory of the IRC for the chemical analysis of the samples.

REFERENCES

1. Chang, C. D., and Silvestri, A. J., *J. Catal.* **47**, 249 (1977).

2. Derouane, E. G., Dejaifve, P., B. Nagy, J., van Hooff, J. H. C., Spekman, B. P., Naccache, C., and Védrine, J. C., *C. R. Acad. Sci. Paris, Ser. C* **284**, 945 (1977); *J. Catal.* **53**, 40 (1978).

3. Argauer, R. J., and Landolt, G. R., U. S. Patent 3,702,886, November 14, 1972.

4. Kokotailo, G. T., Lawton, S. L., Olson, D. H., and Meier, W. M., *Nature (London)* **272**, 437 (1978).

5. Flanigen, E. M., Bennet, J. M., Grose, R. M., Cohen, J. P., Patton, R. L., Kirchner, R. M., and Smith, J. V., *Nature (London)* **271**, 512 (1978).

6. Primet, M., Védrine, J. C., and Naccache, C., *J. Mol. Catal.* **4**, 411 (1978).

7. Abou-Kais, A., Védrine, J. C., Massardier, J., Dalmai-Imelik, G., and Imelik, B., *J. Chim. Phys.* **69**, 561 (1972).
8. Ben Taarit, Y., Naccache, C., and Imelik, B., *J. Chim. Phys.* **70**, 728 (1973).
9. Lotkev, M. I., *Russ. Chem. Rev.* **45**, 1594 (1976).
10. Parry, E. P., *J. Catal.* **2**, 371 (1963).
11. Rudolph, J., and Zimmermann, H., *Z. Phys. Chem. (Frankfurt am Main)* **43**, 311 (1964); Colomban, P., Lucazeau, G., Mercier, R., and Novak, A., *J. Chem. Phys.* **67**, 5244 (1977).
12. Abou-Kais, A., Massardier, J., Dalmai-Imelik, G., and Imelik, B., *J. Chim. Phys.* **69**, 570 (1972).
13. Adrian, F. J., *J. Chem. Phys.* **32**, 972 (1960).
14. Iton, L. E., and Turkevich, J., *J. Phys. Chem.* **82**, 200 (1978).
15. Lunsford, J. H., *J. Phys. Chem.* **72**, 4163 (1968).
16. Edlund, O., Kinell, P. O., Lund, A., and Shimizu, A., *J. Chem. Phys.* **46**, 3679 (1967); Komatsu, T., and Lund, A., *J. Phys. Chem.* **76**, 1727 (1972).
17. Védrine, J. C., Dufaux, M., Naccache, C., and Imelik, B., *J. Chem. Soc. Faraday Trans. I* **74**, 440 (1978).
18. Scofield, J. H., *J. Electron Spectrosc.* **8**, 129 (1976).
19. Kerr, G. T., *J. Phys. Chem.* **71**, 4155 (1967); *J. Catal.* **15**, 200 (1969).
20. Védrine, J. C., Abou-Kais, A., Massardier, J., and Dalmai-Imelik, G., *J. Catal.* **29**, 120 (1973).
21. Ward, J. W., *in* "Zeolite Chemistry and Catalysis" (Rabo, J. A., Ed.), Vol. 171, p. 118 Amer. Chem. Soc., Washington, D. C., 1976.
22. Karge, H., *Z. Phys. Chem. (Frankfurt am Main)* **76**, 133 (1971).
23. Chen, N. Y., *J. Phys. Chem.* **80**, 60 (1976).
24. Eberly, P. E., Kimberlin, C. N., and Voorhies, A., *J. Catal.* **22**, 419 (1971).
25. Cannings, F. R., *J. Phys. Chem.* **72**, 4691 (1968).
26. Ben Taarit, Y., Ph.D. thesis, Lyon, France, 1971.
27. Tsutsumi, K., Kajiwara, H., and Takahaski, H., *Bull. Chem. Soc. Japan* **47**, 801 (1974).
28. Tsutsumi, K., Koh, H. Q., Hagiwara, S., and Takahashi, H., *Bull. Chem. Soc. Japan* **48**, 3576 (1975).
29. Auroux, A., Bolis, V., Wierzchowski, P., Gravelle, P. C., and Védrine, J. C., *J. Chem. Soc. Faraday Trans. I.* in press (1979).
30. Flockhart, B. D., *in* "Surface and Defect Properties of Solids," Vol. 2, p. 69, The Chemical Society, London, 1973.
31. Lunsford, J. H., *J. Catal.* **14**, 379 (1969).
32. Kurita, Y., Sonoda, T., and Sato, M., *J. Catal.* **19**, 82 (1970).